5 APPROXIMATE ANALYTICAL MODEL FOR PREDICTING THE BIT ERROR RATE PERFORMACE OF DISTRIBUTED ARRAYS IN A MULTIPATH ENVIRONMENT

5.1 Introduction

In this chapter an approximate equation for the bit error rate of a distributed array with combined beamforming in multipath environment will be presented. The model is based on an extension of the analytical model presented in [11] for a single array in a multipath environment. Firstly the detail of the derivation of the single array model by [11] will be given. The correlation between elements of an array in a low angular spread environment as a function of the element spacing will be calculated. This will be followed by a comparison of the bit error rate determined with the analytical model and the bit error rate determined with a Monte-Carlo simulation with high correlation between antenna elements, specifically for an angular spread of 5 degrees and an element spacing of 0.5 wavelengths.

The extension of the single array model to the distributed array will then be presented. This will be followed by a comparison of the bit error rate between the analytical model and a Monte-Carlo simulation for the distributed array with 0.5 wavelength element spacing and 5 degree angular spread.

The objective of the analytical BER calculation method is two fold, (1) to show that the analytical method presented by [11] can be extended to distributed arrays, and (2) to verify the Monte-Carlo simulation method used in this thesis to calculate the BER of the distributed arrays.

5.1 Single Array

5.1.1 Analytical Formulation

Assume that the noise and interference signals are uncorrelated in the short term, all antenna branches have the same noise power and the average of the co-variance matrix is

taken over a period much less than the channel coherence time[38]. A total of D signals are present, with one desired signal and D-1 interferers. It is further assumed that there is Rayleigh fading between each signal and each antenna element. The short term covariance matrix $\mathbf{R}_{nn}$ of the array can then be written as (using (55) and Appendix A):

$$\mathbf{R}_{nn} = \frac{1}{N}\sum_{n=1}^{N}\mathbf{X}(n)\,\mathbf{X}^{H}(n) + \sigma_N^2\,\mathbf{I} \tag{141}$$

where n is the symbol number (or data bit number), N is the total number of symbols over which an average is taken between fades, $\mathbf{I}$ is the identity matrix, $\mathbf{X}(n)$ is the received signal vector at the array element outputs (after sampling and conversion to baseband) and σ_n^2 is the noise power at each element. The vector $\mathbf{X}(n)$ is equal to:

$$\mathbf{X}(n) = S_d(n)\,\mathbf{U}_d(n) \tag{142}$$

where $S_d(n)$ is the transmitted signal amplitude and $\mathbf{U}_d$ is the propagation vector of signal d. Because of Rayleigh fading, U_{dm} (fading of d-th signal at m-th antenna element) is a complex Gaussian random variable. The propagation vector varies at the fading rate, but when averaged over the fading, it has a power equal to P_d, where

$$P_1 = P_{des} \tag{143}$$

and

$$P_d = P_{int} \tag{144}$$

for $d \in \{2,3,....,D\}$. The power of the desired user P_{des} is given by:

$$P_{des} = \Gamma[(D-1)\Gamma_n + 1] \tag{145}$$

where Γ is the SINR and Γ_n is the INR. The power of the interferers P_{int} is given by:

$$P_{int} = \Gamma_n\,\sigma_n^2 \tag{146}$$

Without loss of generality, it is assumed that the baseband transmit power of each signal is unity or:

[38] Channel coherence time is the time that the channel remains constant.

$$E\left\{S_d^2(n)\right\}=1 \tag{147}$$

Assuming that the baseband data of the signals are uncorrelated, using (142) in (141) with (147), equation (141) can be written as (see Appendix A):

$$\mathbf{R}_{nn} = \sum_{d=2}^{D} \mathbf{U}_d \mathbf{U}_d^H + \sigma_n^2 \mathbf{I} \tag{148}$$

With optimum combining, the instantaneous SINR at the output of the array is [2]:

$$\eta=\mathbf{U}_1^H \mathbf{R}_{nn}^{-1} \mathbf{U}_1 \tag{149}$$

where $\mathbf{U}_1$ is the array propagation vector of the desired signal (d = 1). The instantaneous SINR η is a random variable that varies at the fading rate. Since $\mathbf{U}_d$, where $d \in \{1,\ldots,D\}$, is a complex Gaussian variable, the multivariate complex Gaussian probability density function of $\mathbf{U}_d$ can be written as [61].

$$p_d(\mathbf{U}_d) = \frac{1}{\pi^M \left|\hat{\mathbf{R}}_d\right|} e^{\left(-\mathbf{U}_d \hat{\mathbf{R}}_d^{-1} \mathbf{U}_d^H\right)} \tag{150}$$

where $|\,|$ denotes determinant and $\hat{\mathbf{R}}_d$ is the covariance matrix averaged over short term (multipath) fading for user d. It is further assumed that the multipath fading between different mobile signals is independent as they arrive at each antenna element (low correlation at each array element between the received multipath components of two or more different mobile signals). In an environment with narrow angular spread and/or closely spaced antenna elements, the fading between elements for the same signal will be correlated. The probability density function of the output signal to interference plus noise ratio η is a joint function of all the array vectors:

$$p(\eta) = p_\eta(\mathbf{U}_1, \mathbf{U}_2 \ldots, \mathbf{U}_D) \tag{151}$$

where $p_\eta()$ is the joint PDF of η. Due to independent fading between different signals, the joint probability density function can be written as the product of the individual PDF's:

$$p(\eta) = p_\eta(\mathbf{U}_1, \mathbf{U}_2 \ldots, \mathbf{U}_D) = \prod_{d=1}^{D} p_\eta(\mathbf{U}_d) \tag{152}$$

In order to calculate the bit error rate, the PDF of the SINR must be determined. This can be found by first determining the characteristic function of p_η through the Laplace transform:

$$\Psi(z)=\int_0^\infty p(\eta)e^{(-z\eta)}\,d\eta \tag{153}$$

Now, since $p(\eta) = 0$ for $\eta < 0$, (153) may be written as:

$$\Psi(z)=\int_{-\infty}^\infty p(\eta)e^{(-z\eta)}\,d\eta \tag{154}$$

This equation is actually just the expected value of $e^{(-z\eta)}$ [62]. Inserting now (149) and (152) in (154) we get

$$\Psi(z)=\int_{-\infty}^\infty\!\!\ldots\ldots\int_{-\infty}^\infty\left\{p_\eta(\mathbf{U}_1,\mathbf{U}_2\ldots,\mathbf{U}_D)\,e^{(-z\mathbf{U}_1\mathbf{R}_{nn}^{-1}\mathbf{U}_1^H)}\right\}d\mathbf{U}_1\,d\mathbf{U}_2\ldots..\,d\mathbf{U}_D \tag{155}$$

which can be re-written using (152) as:

$$\Psi(z)=\int_{-\infty}^\infty\!\!\ldots\ldots\int_{-\infty}^\infty\left\{p_\eta(\mathbf{U}_1)\;p_\eta(\mathbf{U}_2)\ldots..p_\eta(\mathbf{U}_D)\right\}d\mathbf{U}1\,d\mathbf{U}_2\ldots..\,d\mathbf{U}_D\;G(z,\mathbf{U}_1,\ldots,\mathbf{U}_D) \tag{156}$$

where

$$G(z,\mathbf{U}_1,\ldots,\mathbf{U}_D)=\int_{-\infty}^\infty p_\eta(\mathbf{U}_1)\,e^{(-z\mathbf{U}_1\mathbf{R}_{nn}^{-1}\mathbf{U}_1^H)}d\mathbf{U}_1 \tag{157}$$

Inserting (150) in (157) we have [11]

$$G(z,\mathbf{U}_2,\ldots,\mathbf{U}_D)=\frac{1}{\pi^M\left|\hat{\mathbf{R}}_1\right|}\int_{-\infty}^\infty p_\eta(\mathbf{U}_1)\,e^{[-\mathbf{U}_1(\hat{\mathbf{R}}_1^{-1}+z\mathbf{R}_{nn}^{-1})\mathbf{U}_1^H]}d\mathbf{U}_1 \tag{158}$$

It is shown in [11] that the definite integral in (158) is:

$$\int_{-\infty}^\infty e^{(-\mathbf{x}\mathbf{A}\mathbf{x}^H)}d\mathbf{x}=\frac{\pi^M}{|\mathbf{A}|} \tag{159}$$

Using (159) in (158), the following is obtained:

$$G(z, \mathbf{U}_2, \ldots, \mathbf{U}_D) = \frac{1}{\pi^M \left|\hat{\mathbf{R}}_1\right|} \frac{\pi^M}{\left|\hat{\mathbf{R}}_1^{-1} + z\mathbf{R}_{nn}^{-1}\right|} = \frac{1}{\left|\mathbf{I} + z\hat{\mathbf{R}}_1 \mathbf{R}_{nn}^{-1}\right|} \tag{160}$$

Now $G(z, \mathbf{U}_2, \ldots, \mathbf{U}_D)$ can be re-written as follows:

$$G(z, \mathbf{U}_2, \ldots, \mathbf{U}_D) = G(z, \lambda_1, \ldots, \lambda_M) = \frac{1}{\left|\prod_{m=1}^{M}\left(1+\frac{z}{\lambda_m}\right)\right|} = \prod_{m=1}^{M}\left(\frac{\lambda_m}{z+\lambda_m}\right) \tag{161}$$

where $\lambda_1, \lambda_2, \ldots, \lambda_M$ are the eigenvalues of $\left(\hat{\mathbf{R}}_1 \mathbf{R}_{nn}^{-1}\right)^{-1} = \mathbf{R}_{nn} \hat{\mathbf{R}}_1^{-1}$. The eigenvalues are the solutions to the generalized eigenvalue problem:

$$\mathbf{R}_{nn}\, \mathbf{v} = \lambda \hat{\mathbf{R}}_1\, \mathbf{v} \tag{162}$$

where $\mathbf{v}$ are the eigenvectors. The average of a function g(x) is per definition [62]:

$$E[g(x)] = \int_{-\infty}^{\infty} p(x)\, g(x)\, dx \tag{163}$$

where p(x) is the probability density function of x. Using (163) in (156), the characteristic function $\Psi(z)$ is actually the average of $G(z, \lambda_1, \ldots, \lambda_M)$. It is shown in [11] that the characteristic function can be approximated by:

$$\Psi(z) = \prod_{m=1}^{M}\left(\frac{\langle\lambda_m\rangle}{z+\langle\lambda_m\rangle}\right) \tag{164}$$

where $\langle\lambda\rangle$ is the mean of the eigenvalue. In the case where there is uncorrelated fading between elements for the same signal (large element spacing or wide angular spread), the interference plus noise co-variance matrix simplifies significantly [11]. There are M-1 eigenvalues equal to zero and one non-zero eigenvalue. The BER for this simplified case is given in Appendix C. In the case of all unique eigenvalues (multiplicity equal to one),

which is typically the case when a signal is correlated between antenna branches, a partial fractional expansion of the characteristic function in (164) is given by:

$$\Psi(z)=C\left[\frac{\Omega_1}{(z+\lambda_1)}+\frac{\Omega_2}{(z+\lambda_2)}+....+\frac{\Omega_M}{(z+\lambda_M)}\right] \tag{165}$$

which is equal to:

$$\Psi(z)=C\sum_{m=1}^{M}\left[\frac{\Omega_m}{(z+\lambda_m)}\right] \tag{166}$$

with

$$\Omega_m=\frac{1}{\prod_{i=1,i\neq m}^{M}(\lambda_m-\lambda_i)} \tag{167}$$

and

$$C=\prod_{m=1}^{M}\lambda_m \tag{168}$$

Now, the probability density function $p(\eta)$ is the inverse Laplace transform of the characteristic function in (166), given by:

$$p(\eta)=L^{-1}\{\Psi(z)\}=C\sum_{M=1}^{M}\Omega_m e^{-\lambda_m\eta} \tag{169}$$

The average (over Rayleigh fading) bit error rate (BER) of phased shift keyed signals is given by [11]:

$$BER=\tfrac{1}{2}\int_{-\infty}^{\infty}p(\eta)\,\mathrm{erfc}(\sqrt{\eta})\,d\eta \tag{170}$$

Inserting (169) in (170), the following is obtained:

$$BER=\frac{C}{2}\int_{-\infty}^{\infty}\sum_{m=1}^{M}\left(\Omega_m e^{-\lambda_m\eta}\right)\mathrm{erfc}(\sqrt{\eta})\,d\eta \tag{171}$$

The following general integral formula [11] is used to evaluate (171):

$$\frac{1}{2}\int_0^{\infty} e^{(-a\,x)}\ \mathrm{erfc}(\sqrt{bx}\,dx = \frac{\sqrt{1+\frac{a}{b}}-1}{2a\sqrt{1+\frac{a}{b}}} \tag{172}$$

Finally, using (172) in (171), the average bit error rate is:

$$BER = C\sum_{m=1}^{M}\Omega_m\left(\frac{\sqrt{1+\lambda_m}-1}{2\lambda_m\sqrt{1+\lambda_m}}\right) \tag{173}$$

5.1.2 Single Array Result with Correlated Fading

In order to calculate the bit error rate in (173) the eigenvalues must be determined. It was shown in [11] that the average eigenvalues in the case of uncorrelated fading across the elements can be determined with a Monte-Carlo simulation. In the case of correlated fading between elements, the eigenvalues must be calculated for each interference to noise level. An example of the eigenvalues for one interferer and equal INR and SNR of 20dB was presented in [11] for a correlation value of 0.9.

The performance of closely spaced antenna elements (0.5λ[39]) of distributed arrays in low to moderate multipath environments is investigated in this thesis. The correlation between elements is a function of the element spacing, angular spread and mean incidence angle [25]. A low correlation between elements improves the array's ability to discriminate in the spatial domain between various incoming multipath components. Therefore, it is important to quantify the correlation between elements as function of spacing and angular spread.

The average correlation between the elements of a two-element array is:

$$\text{Correlation} = \frac{\hat{\mathbf{R}}_1(1,2)}{\sqrt{\hat{\mathbf{R}}_1(1,1)\,\hat{\mathbf{R}}_1(2,2)}} \tag{174}$$

where $\hat{\mathbf{R}}_1(n,m)$ is the covariance matrix of elements n and m averaged over short term fading. The correlation as a function of the element spacing was calculated for an angular

[39] This is the typical antenna spacing used in scanning arrays to avoid grating lobes.

spread of 5°, zero mean incidence angle and with a SNR = INR = 10dB. The calculated eigenvalues for one interferer is given in Table 8 with averaging over 4000 iterations. The eigenvalues is the solution of the generalized eigenvalue problem given in (162). The Rayleigh fading model in section 2.4.1.1.2 is used with 30 scatterers to generate the signals at the antenna elements, which is then applied to calculate the co-variance matrices. The eigenvalues decrease with an increase in element spacing. The correlation as a function of the element spacing is shown in Figure 49. This figure indicates, for example, that there is a 50% correlation between elements with an interelement spacing of 4.2λ. Furthermore, it can be seen that there is a correlation of more than 98% between elements when the interelement spacing is 0.5λ.

Table 8: Eigenvalues as a function of the interelement spacing.

Element Spacing [wavelengths]	$\langle\lambda_1\rangle$	$\langle\lambda_2\rangle$
0.2	1.040985	68.89308
0.6	0.985893	8.462671
1.0	0.865898	3.984874
1.8	0.589558	2.318541
3.0	0.439151	1.973366
4.2	0.375803	1.885298
5.0	0.36517	1.870526
6.2	0.34629	1.865329
7.0	0.349004	1.852482
7.8	0.35091	1.877462

Using equation (173), the analytical BER is compared in Figure 50 to that calculated with a Monte-Carlo simulation with the signals in a Rayleigh fading environment. The fading environment is generated with 30 scatterers according to the Rayleigh method described in section 2.4.1.1.2. The configuration is a two-element array with two equal power interferers and an INR of 2. The element spacing is 0.5λ, angular spread is 5° and the number of scatterers is 30. The mean eigenvalues over 2000 iterations is given in Table 9. It can be seen from Figure 50 that there is good agreement between the analytical and the Monte-Carlo simulation results.

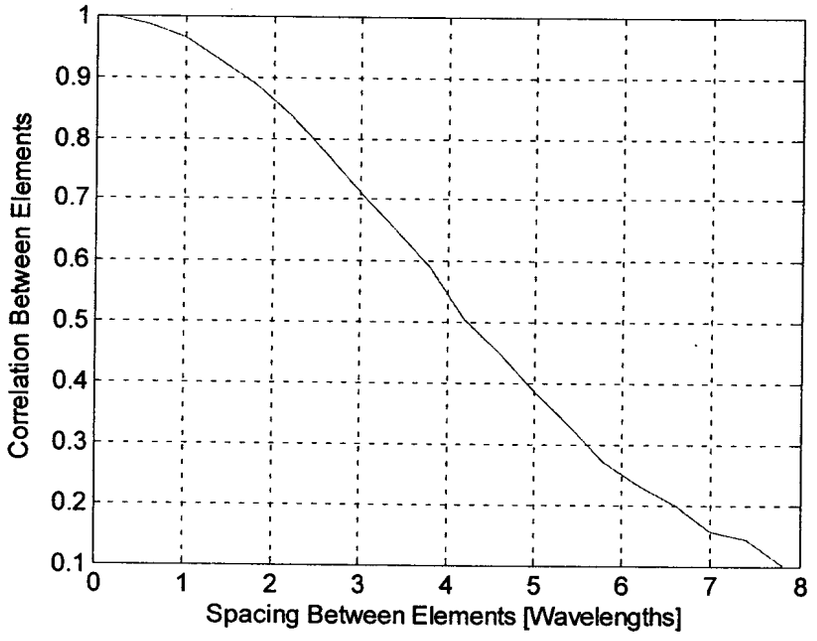

Figure 49: Correlation between two antenna elements as a function of the inter-element spacing for an angular spread of 5°.

Table 9: Mean eigenvalues of a two-element array in the presence of two interferers.

SINR [dB]	$\langle\lambda_1\rangle$	$\langle\lambda_2\rangle$
-10	14.737	375.48
-8	9.094	240.486
-6	6.152	152.195
-4	3.875	92.117
-2	2.492	55.913
0	1.473	37.859
2	0.933	24.089
4	0.604	14.979
6	0.385	9.907
8	0.244	5.815
10	0.147	3.808
12	0.098	2.347
14	0.059	1.424

SINR [dB]	$\langle\lambda_1\rangle$	$\langle\lambda_2\rangle$
16	0.038	0.82
18	0.024	0.628
20	0.014	0.37

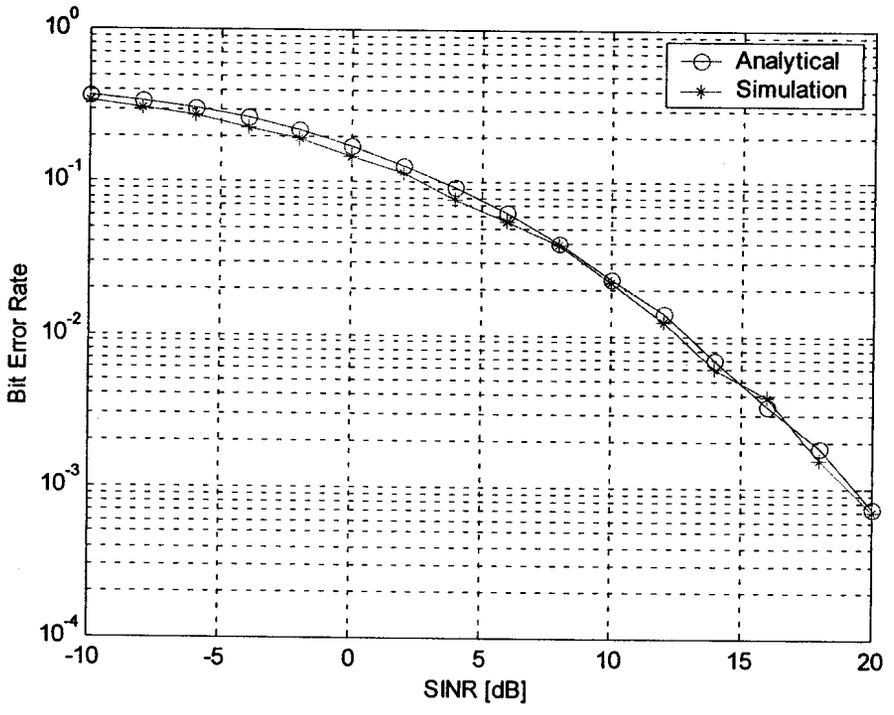

Figure 50: Analytical BER compared to BER calculated with Monte-Carlo simulations with signals in a Rayleigh fading environment for a two-element array with two equal power interferers.

5.2 Distributed Array

In this section an analytical expression will be derived for the bit error rate of a distributed array with combined beamforming in a fast fading environment based on the method of the single array presented in the previous section.

5.2.1 Analytical Formulation

Assume that the noise and interference signals are uncorrelated in the short term, all elements of the three sub-arrays have the same noise power and the average of the interference correlation matrix is taken over a period much less than the channel coherence time. The short term covariance matrix of the interference plus noise of the combined

distributed array (consisting of all three sub-arrays with combined beamforming) $\ddot{\mathbf{R}}_{nn}$ can then be written as:

$$\ddot{\mathbf{R}}_{nn} = \frac{1}{N}\sum_{n=1}^{N}\sum_{d=1}^{D}\ddot{\mathbf{X}}_d(n)\,\ddot{\mathbf{X}}_d^H(n) + \sigma_N^2\,\mathbf{I} \tag{175}$$

where n is the symbol number (or bit number), N is the total number of symbols (or data bits) over which an average is taken, $\mathbf{I}$ is the identity matrix spanning all three sub-arrays, $\ddot{\mathbf{X}}(n)$ is the combined received signal vector of all three sub-arrays and σ_N^2 is the noise power at each element of the combined array. The vector $\ddot{\mathbf{X}}(n)$ is equal:

$$\ddot{\mathbf{X}}(n) = S_d(n)\,\ddot{\mathbf{U}}_d(n) \tag{176}$$

where $S_d(n)$ is the transmitted signal amplitude and $\ddot{\mathbf{U}}_d$ is the propagation vector of signal d at the combined array (given in (1) for the uniform linear array). The propagation vector varies at the fading rate, but when averaged over the fading, it has a power at each element of sub-array $\kappa \in \{1,2,3\}$ equal to $P_{d,\kappa}$, where

$$P_{1,\kappa} = \frac{P_{des}}{\left(\frac{r_{1,\kappa}}{r_{1,\kappa}^{pc}}\right)^{\gamma}} \tag{177}$$

and

$$P_{d,\kappa} = \frac{P_{int}}{\left(\frac{r_{d,\kappa}}{r_{d,\kappa}^{pc}}\right)^{\gamma}} \tag{178}$$

for $d \in \{2,3,....,D\}$. $r_{d,\kappa}$ is the range between the sub-array and mobile d and $r_{d,\kappa}^{pc}$ is the power control radius (see section 2.5.5). The power of the desired user P_{des} is given by:

$$P_{des} = \Gamma\left[(D-1)\Gamma_n + 1\right] \tag{179}$$

where Γ is the SINR and Γ_n is the INR. The power of the interferers P_{int} is given by:

$$P_{int} = \Gamma_n\,\sigma_n^2 \tag{180}$$

Assume without loss of generality that:

$$E\left\{S_d^2(n)\right\}=1 \tag{181}$$

Assuming that the signal data are uncorrelated and using (181), (175) can be written as (see Appendix A):

$$\ddot{\mathbf{R}}_{nn} = \sum_{d=1}^{D} \ddot{\mathbf{U}}_d \, \ddot{\mathbf{U}}_d^H + \sigma_N^2 \mathbf{I} \tag{182}$$

With optimum combining, the instantaneous SINR at the output of the array is [2]:

$$\eta = \ddot{\mathbf{U}}_1 \, \ddot{\mathbf{R}}_{nn}^{-1} \, \ddot{\mathbf{U}}_1^H \tag{183}$$

where $\ddot{\mathbf{U}}_1$ is the combined propagation vector of the desired signal (d = 1) The instantaneous signal to interference plus noise ratio η is a random variable that varies at the fading rate. The multivariate Gaussian density function of $\mathbf{U}_d$, where d $\in$ {1,2,...D}, can be written as [61].

$$p_d(\ddot{\mathbf{U}}_d) = \frac{1}{\pi^M \left|\ddot{\hat{\mathbf{R}}}_d\right|} e^{\left(-\ddot{\mathbf{U}}_d \ddot{\hat{\mathbf{R}}}_d^{-1} \ddot{\mathbf{U}}_d^H\right)} \tag{184}$$

where | | denotes determinant and $\ddot{\hat{\mathbf{R}}}_d$ is the co-variance matrix averaged over short term (multipath) fading. All signals are assumed to have independent scattering, but the fading for each signal may be correlated between the array elements (due to coupling between closely spaced elements, narrow angular spread or mutual coupling). Furthermore, it is assumed that the fading between the sub-arrays are uncorrelated[40]. The rest of the derivation is similar to the single element derivation. Following the same derivation as for the single element case (see section 5.1), the characteristic function $\Psi(z)$ can be approximated by:

$$\Psi(z) = \prod_{m=1}^{M*K} \left(\frac{\langle \lambda_m \rangle}{z + \langle \lambda_m \rangle} \right) \tag{185}$$

[40] This is a valid assumption since the arrays are located far apart.

where $\langle\lambda\rangle$ is the average value of the eigenvalue, determined for the combined array. The total number of eigenvalues is the number of elements multiplied by the number of sub-arrays. With correlation between the elements, the eigenvalues are unique and the BER is given by (using equations (173), (167) and (168)):

$$BER = C\sum_{m=1}^{M*K}\Omega_m\left(\frac{\sqrt{1+\lambda_m}-1}{2\lambda_m\sqrt{1+\lambda_m}}\right) \tag{186}$$

where

$$\Omega_m = \frac{1}{\prod_{i=1,i\neq m}^{M*K}(\lambda_m-\lambda_i)} \tag{187}$$

and

$$C = \prod_{m=1}^{M*K}\lambda_m \tag{188}$$

5.3 Distributed Array Results

In this section the BER calculated with the analytical method is compared to that determined with a Monte-Carlo simulation. A two-element sub-array with two equal strength interferers is considered. The interferers and desired signal are all co-located (worst case) at the following location (see Figure 51):

$$x = 0.5r\cos(30^\circ) = 433\,m \tag{189}$$

and

$$y = 0.5r\sin(30^\circ) = 250\,m \tag{190}$$

The interference to noise ratio is two, angular spread is 5° and the element spacing is 0.5λ. Sub-array 1 is controlling the power (according to the range power control in 2.5.5.1) with a control radius of 620m. The range between mobile and sub-array 2 is 1118m and sub-array 3 is 1454m. The mean eigenvalues calculated with a Monte-Carlo simulation (see section 2.9.1) is given in Table 10. The pathloss exponent is 3.

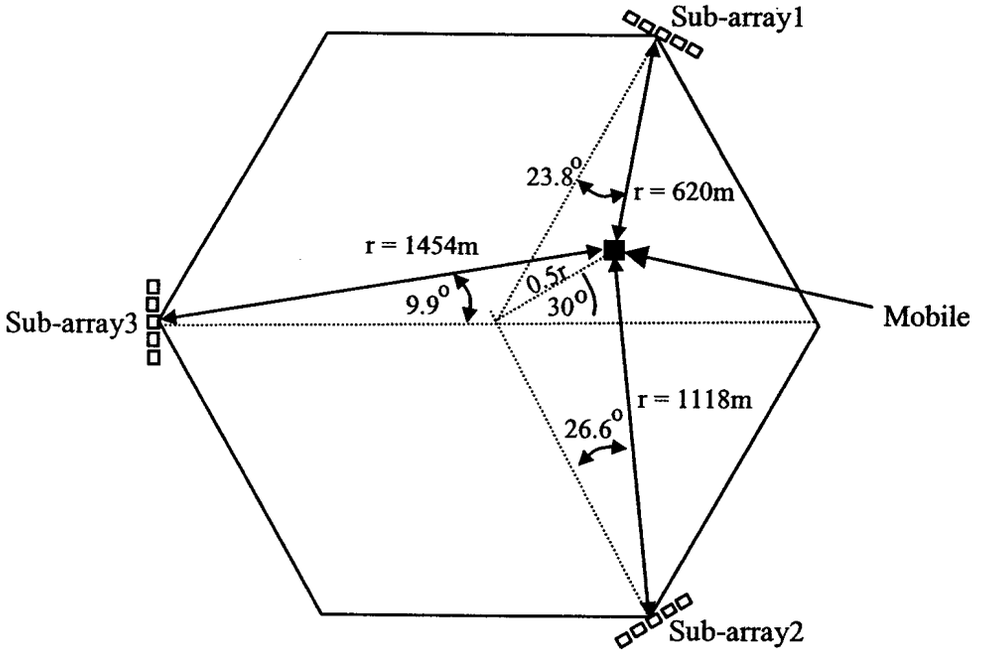

Figure 51: Location of mobiles.

Table 10: Mean Eigenvalues.

SINR [dB]	$\langle\lambda_1\rangle$	$\langle\lambda_2\rangle$	$\langle\lambda_3\rangle$	$\langle\lambda_4\rangle$	$\langle\lambda_5\rangle$	$\langle\lambda_6\rangle$
-10	4.752	15.688	51.227	425.35	3148.572	5228.268
-8	2.84	10.123	33.49	295.658	1798.889	3427.399
-6	1.665	6.537	21.343	169.93	1083.352	1978.911
-4	1.028	3.834	12.88	106.052	692.569	1201.742
-2	0.687	2.168	7.476	69.717	391.569	780.536
0	0.447	1.468	4.858	43.794	295.103	422.912
2	0.289	0.956	3.116	26.505	176.979	353.787
4	0.179	0.623	2.102	16.49	91.783	206.547
6	0.111	0.414	1.367	11.177	69.362	136.821
8	0.082	0.271	0.896	7.322	39.695	79.587
10	0.045	0.148	0.492	4.596	23.218	45.585

A comparison between the BER determined with the analytical method compared to the BER determined with a Monte-Carlo simulation is shown in Figure 52. It can be seen that there is excellent agreement between the two methods.

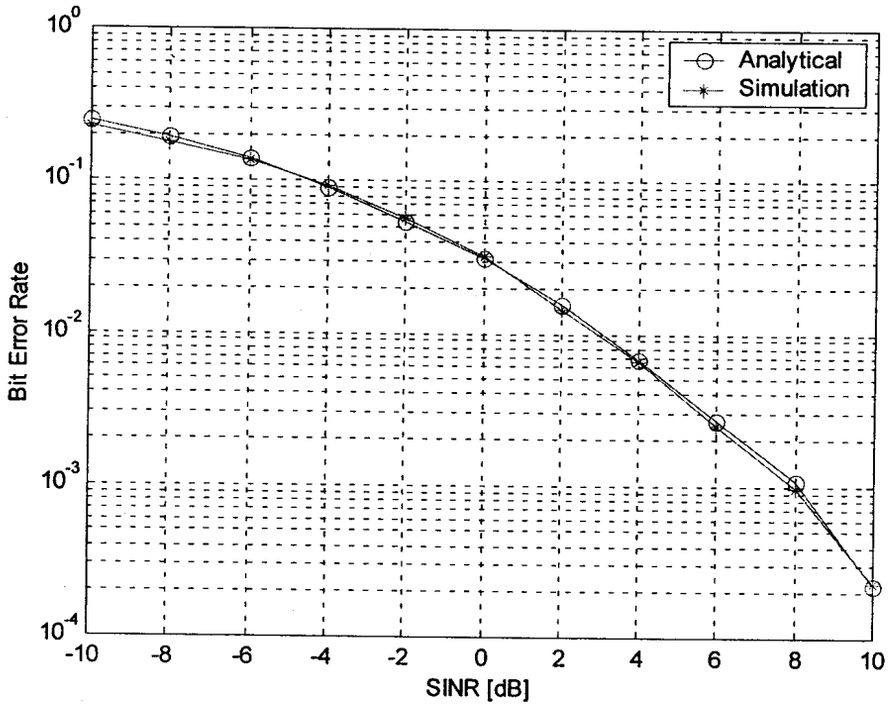

Figure 52: Analytical vs. Monte-Carlo BER comparison for a two-element array with two interferers.

The BER will be lower when the two signals are not co-located. The above result shows the worst case BER as a function of signal to noise ratio.

5.4 Conclusions

An analytical approximation for the bit error rate of a distributed array in a fast fading multipath environment was derived in this chapter. This derivation is based on an extension of a known derivation for the analytical BER of multipath signals received at a single array. The analytical method basically determines a characteristic function as the Laplace transform of the joint multivariate Gaussian probability density function for independent fading between signals. A generalized eigenvalue problem is then solved to determine the eigenvalues of the characteristic function. Once this is known, the characteristic function can be inverted to determine the probability density function. With

this probability function known, the BER can be determined in closed form for phased shift keyed signals.

In order to test the analytical approximation, the bit error rate of a distributed array with half wavelength element spacing was compared to the bit error rate calculated with a Monte-Carlo estimation for two co-located mobiles in a 5° angular spread environment. There are good agreement between the results.

6 DISTRIBUTED ARRAY PERFORMANCE IN A MULTIPATH ENVIRONMENT

6.1 Introduction

The ability of an array to reduce the interference from mobiles with incidence angles close to the desired signal incidence angle, is a function of the angular spread and the distance between array elements. An array with a large element spacing (5λ) and moderate angular spread (5°) or an array with a small element spacing (0.5λ) and wide angular spread (30°) is able to significantly reduce the signal from an interferer closely separated in incidence angle (even equal incidence angles) to that of the desired signal.

Distributed arrays offers an improvement in interference signal rejection relative to conventional arrays at the cell center for signals operating in a moderate multipath environment with closely spaced antenna elements (0.5λ). In the first part of this chapter, the performance (in terms of bit error rate) of a single array will be investigated as a function of the number of elements, the element spacing and the angular spread.

The performance of distributed arrays located at the edges of the cell will then be investigated as a function of the number of elements, element spacing and angular spread. A seven cell network will be considered.

The distributed array performance with combined beamforming (combined weight vector for all sub-arrays) will be compared to arrays with individual beamforming (individual weight vector for all sub-arrays).

The uplink performance of TDMA systems is the focus of the investigation in this chapter. The downlink performance of combined beamforming vs. independent beamforming of adaptive arrays in the CDMA downlink during soft handoff will be investigated in chapter 1.

6.2 Simulation Method and General Parameters

The array element pattern that is used in the simulations is a standard 120° pattern, as shown in Figure 8. The bit error rate for each mean SINR is evaluated with Monte-Carlo simulations over 20 000 iterations (unless stated otherwise), using equation (63). The circular vector channel model with 30 scatterers (K=30) is used and the interferer to noise ratio is 2 [or 3dB]. A diagram of the simulation procedure is shown in Figure 53.

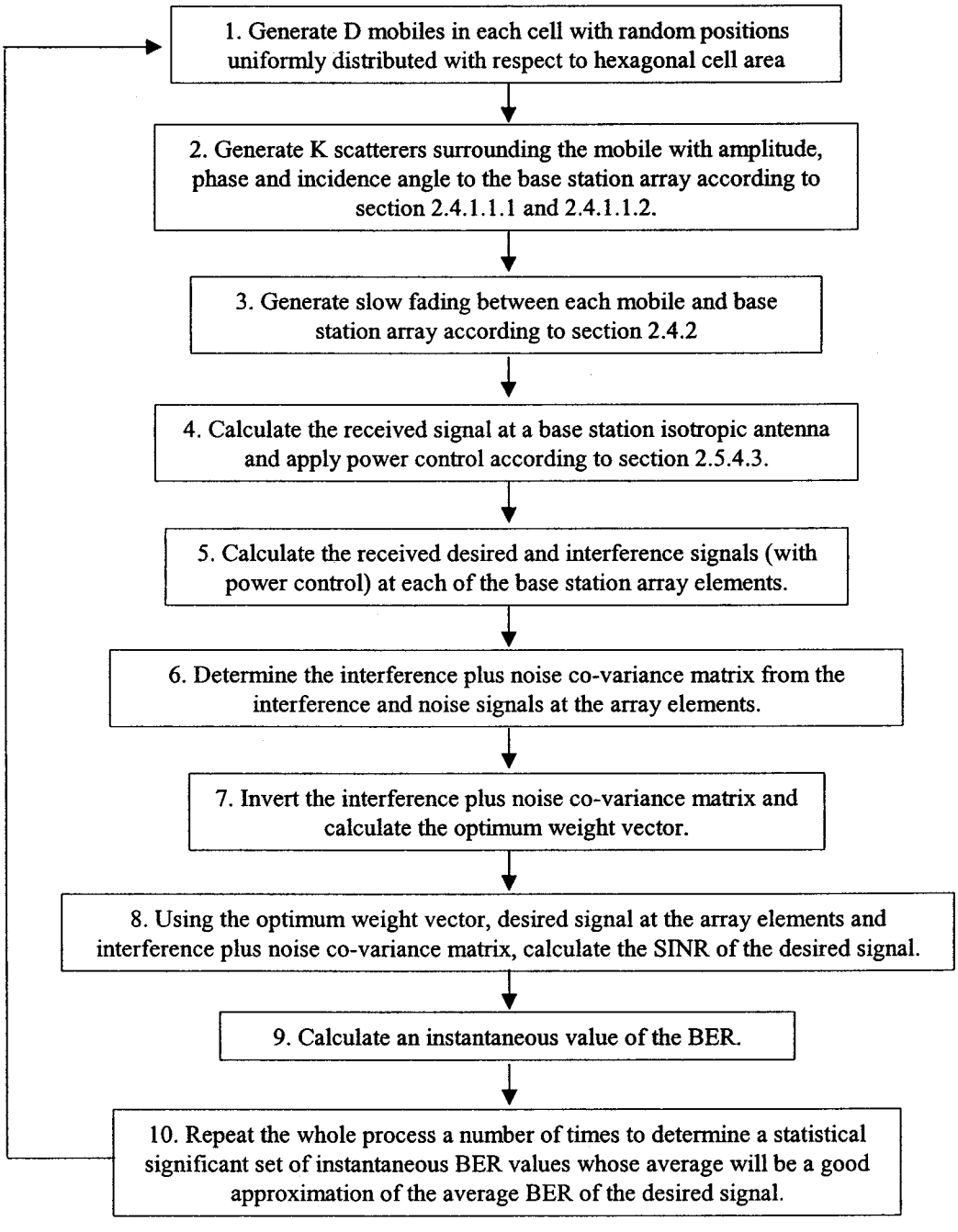

Figure 53: Diagram of the individual simulation steps.

6.2.1 Verification of software code

In this section the accuracy of the implemented simulation program code (based on the formulation in chapter 1) is verified. The calculated BER for two and three element arrays is shown in Figure 54. This is compared to the numerical Monte-Carlo results given in [2] for the case with two equal power interferers. Similar results can be found in [11], where the BER was calculated with an analytical method. The element spacing is 5λ and the multipath scattering angle is 20°. This spacing and angular spread results in uncorrelated or independent fading between antenna elements [25]. The desired signal and interferer are at the same location (therefore the mean incidence angle as seen from the array is the same for both)

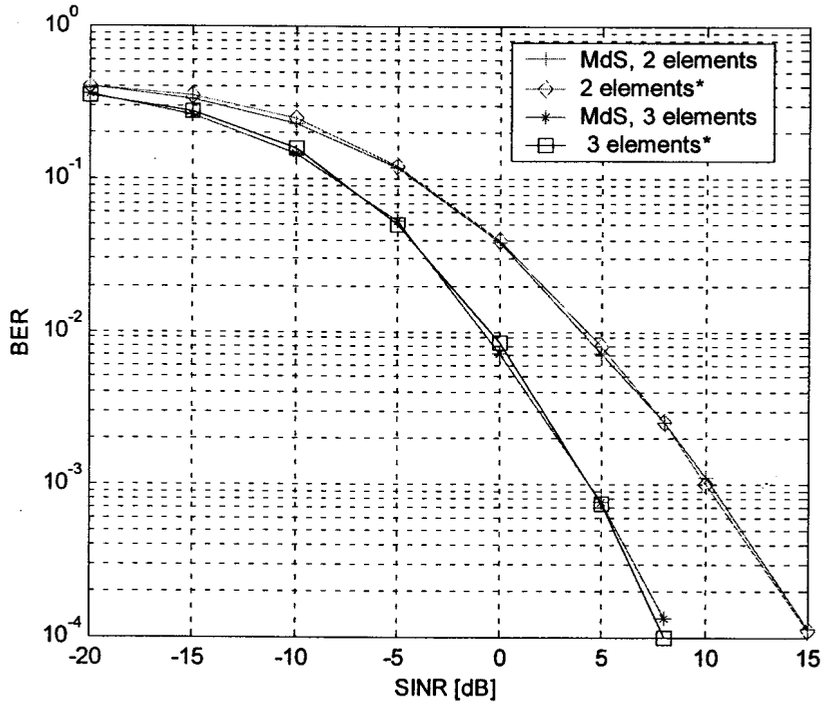

Figure 54: Comparison of results with [2] for a single array with two or three elements and two equal power interferers. * From reference [2].

It can be seen in Figure 54 that there is excellent agreement between the results obtained here and the results in [2], verifying that the software code is accurate.

6.2.2 BER of Circular Vector Channel Model vs. Rayleigh Fading

A comparison between the BER calculated using the circular vector channel model and Rayleigh fading model (see section 2.4.1.1.2) is shown in Figure 55. The configuration is

a two element array with one interferer and interference to noise ratio of 2. An element spacing of 0.5λ and 5λ is considered, and the scattering angle is 5° in both cases. The circular vector channel model gives a higher BER than Rayleigh fading for SINRs above 5dB.

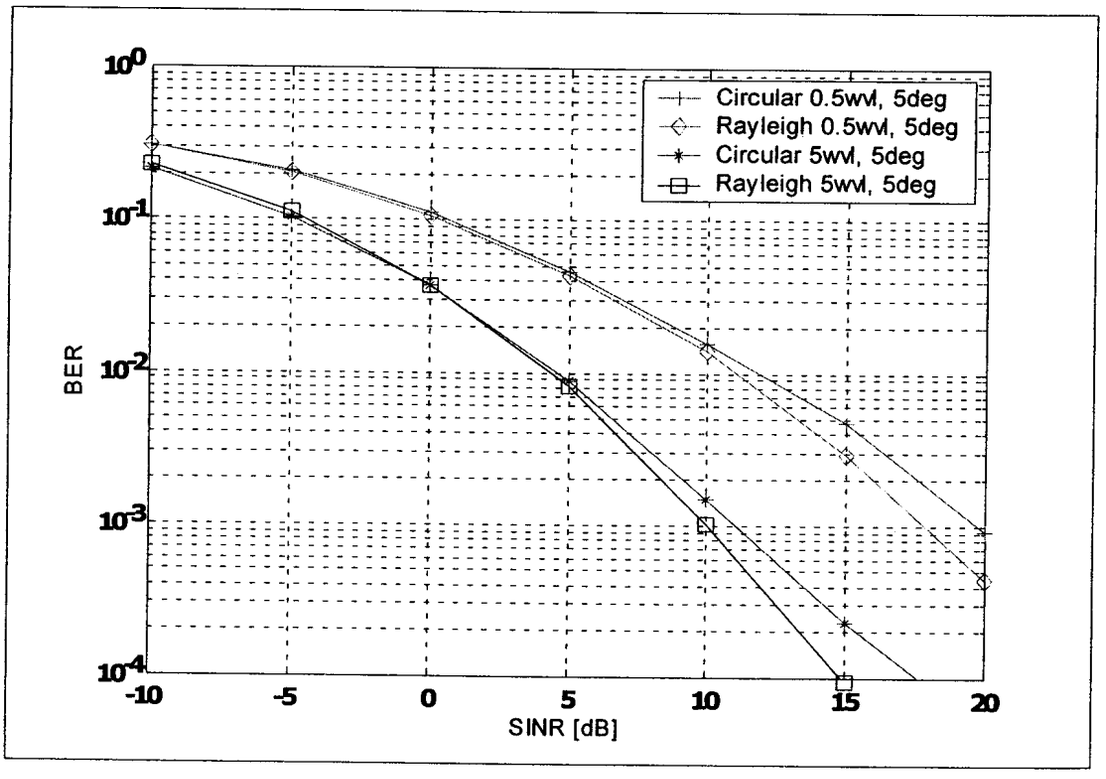

Figure 55: Circular vector channel model vs. Rayleigh fading.

6.2.3 BER vs. Number of Elements (Fixed Element Spacing and Scattering Angle)

The bit error rate versus the number of antenna elements in a rich multipath environment, with large element spacing and one interferer in the same direction as the desired signal, is shown in Figure 56. The array spacing is 5λ and the angular spread is 30°. The figure shows that as the number of elements is increased, the BER is reduced. This is due to improved reduction of the interference multipath components and therefore an increase in the signal to interference plus noise ratio.

6.2.4 BER vs. Scattering Angle

The bit error rate as a function of the SINR and angular spread is shown in Figure 57 for one interferer and in Figure 58 for two interferers in the same direction as the desired signal. The element spacing is 0.5λ and a four element array is considered. The figures

show that as the scattering angle increases, the BER reduces due to improved cancellation of the interference multipath components.

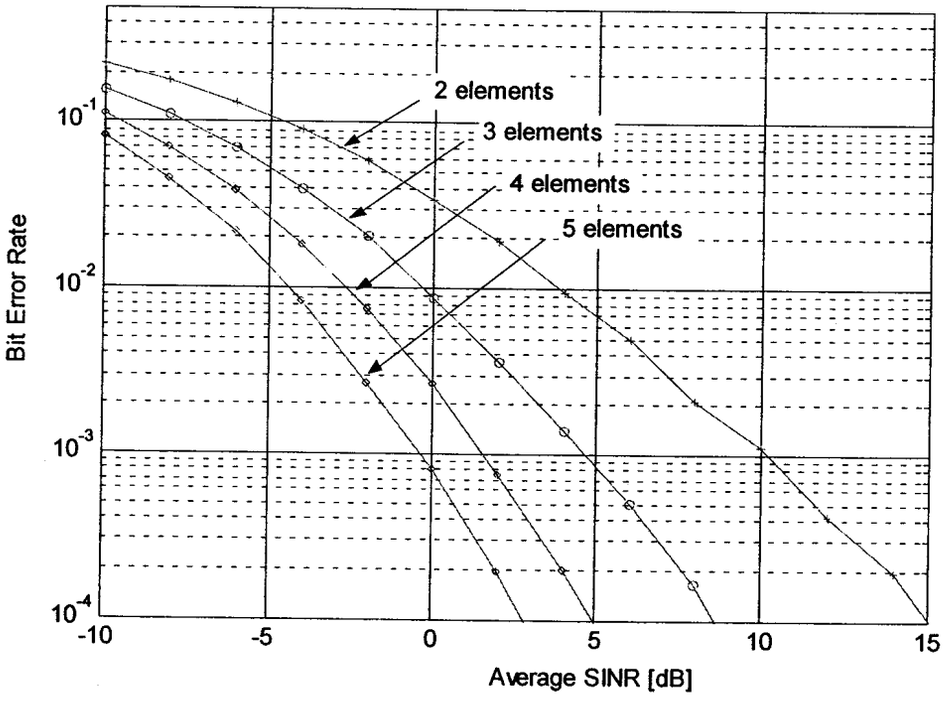

Figure 56: BER as a function of SINR and number of elements with one interferer.

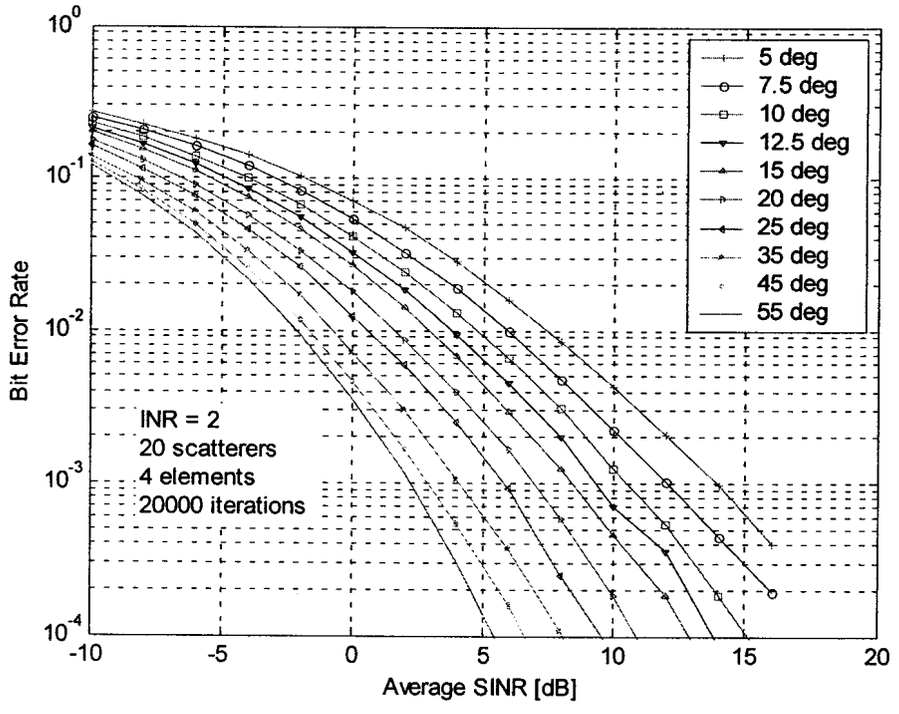

Figure 57: BER as a function of SINR and angular spread with one interferer.

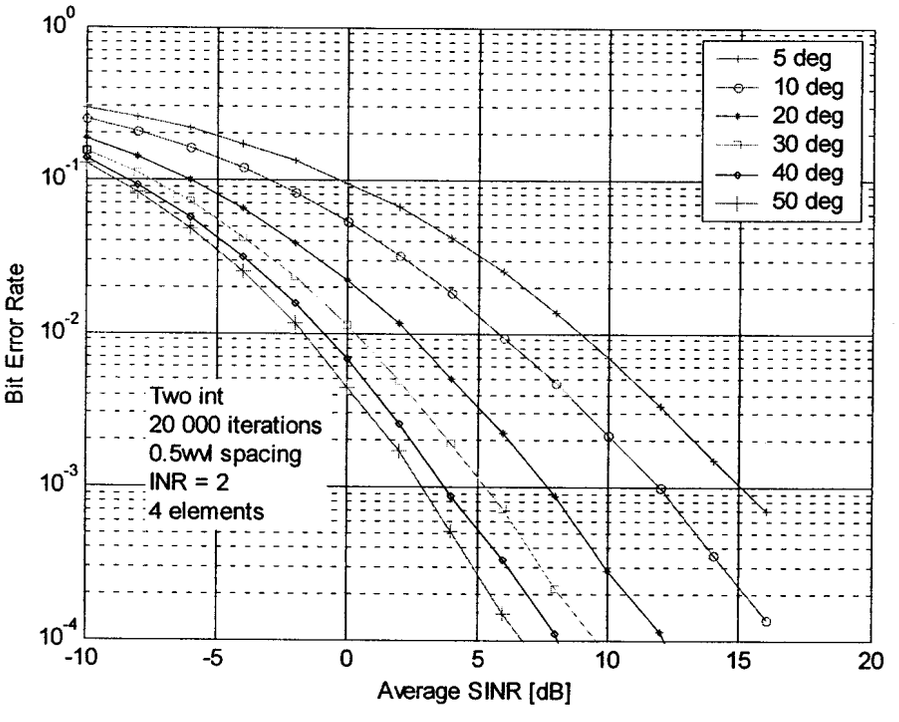

Figure 58: BER as a function of SINR and angular spread with two interferers.

6.3 Distributed Array (Arrays at the Edges of the Cell)

In this section the bit error rate of three distributed arrays at alternate edges of the cell is investigated. The geometry of the distributed array as well as desired and interfering mobiles is shown in Figure 59)

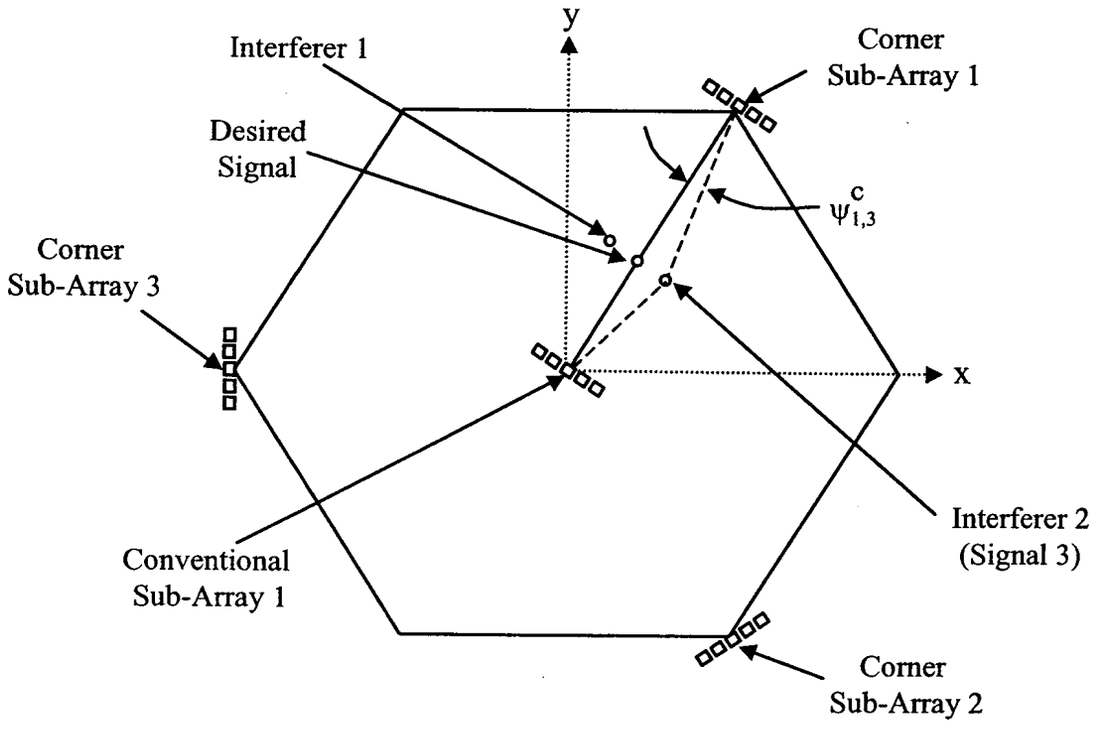

Figure 59: Locations of the desired and interfering signals.

6.3.1 Combined vs. Independent Adaptive Beamforming

The BER of the combined beamforming array vs. the minimum BER of the three independent arrays as a function of the angular spread is shown in Figure 60. The number of array elements is two and two equal power interferers are present. The incidence angles of the desired and interfering signals are all equal and range power control is assumed. It can be seen that the BER of the distributed arrays with independent beamforming is significantly higher than the BER of the combined array. In addition it can be seen that the BER of the independent beamforming arrays decreases as the angular spread increases, as

was also observed for the single four element array in Figure 58. The BER of the combined array on the other hand reduces only slightly as the angular spread increases[41].

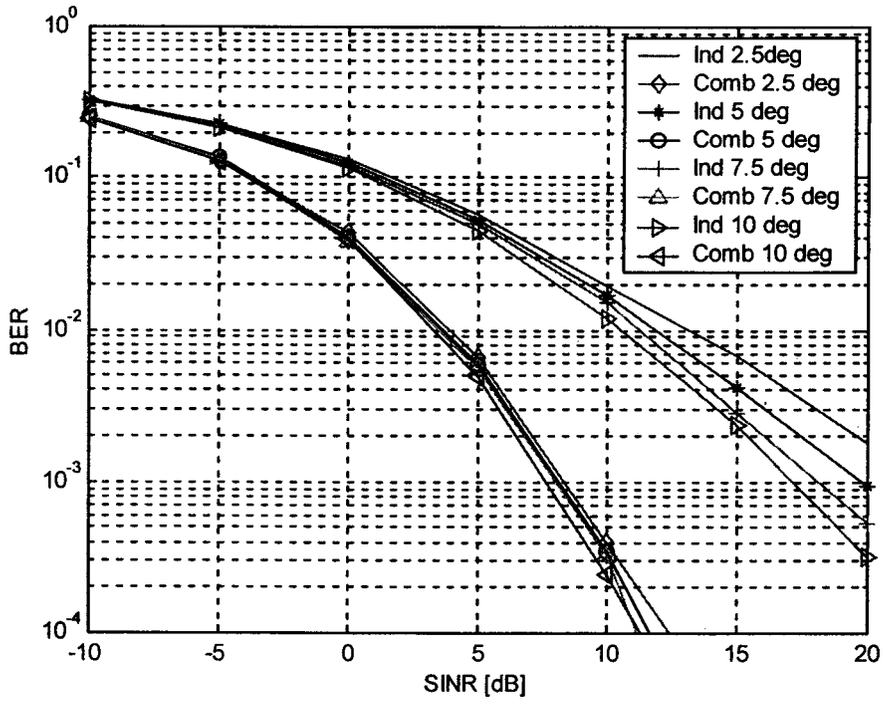

Figure 60: BER of independent vs. combined arrays as a function of angular spread for 2 element arrays.

The BER as a function of the SINR for the desired signal and interferers separated in angle by 5° is shown in Figure 61 for two element arrays with an angular spread of 5° and 10°. Comparing this to Figure 60, it can be seen that the results are very similar. This is to be expected, since the arrays has only two elements with a wide Fresnel beamwidth.

[41] Note that the conventional array BER is the same as the minimum BER of the distributed arrays with independent beamforming.

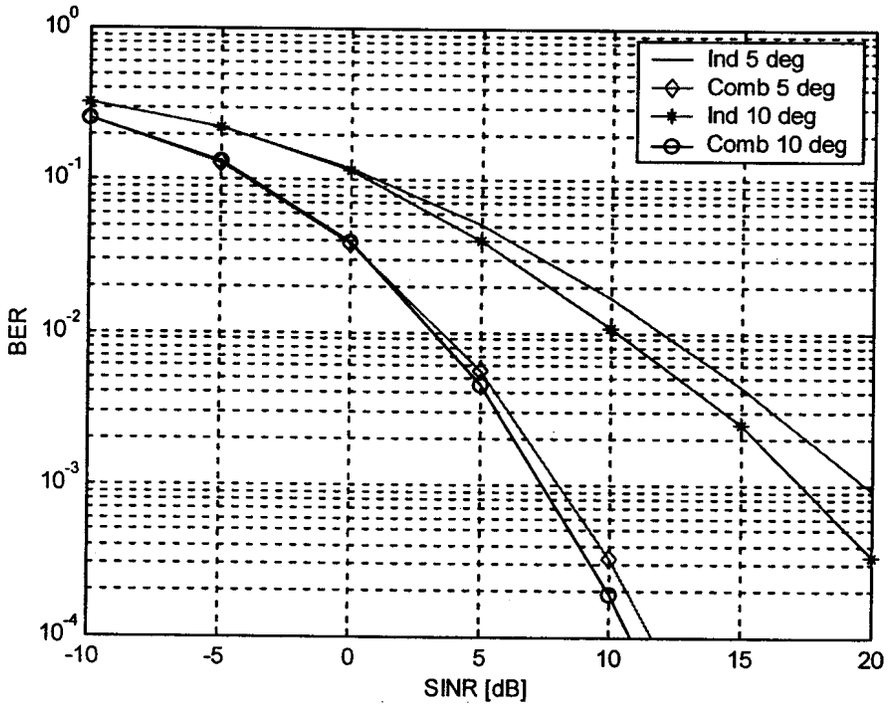

Figure 61: BER as a function of the SINR of independent vs. combined beamforming for two-element arrays with two interferers. The interferers are separated by 5° in angle relative to the desired signal.

The BER as a function of the SINR and angular spread for the center arrays and corner arrays with independent and combined beamforming for a four element array and two equal strength interferers is shown in Figure 62 with the interferers in the same direction as the desired signal. The case where the interfering signals are 5° in angle on both sides of the desired signal (see Figure 59) is shown in Figure 63. Comparing the two cases (Figure 62 and Figure 63), it can be seen that the resolution of the array is only sufficient to achieve a small reduction in the interference and therefore a slight reduction in the BER when the interferers are separated in incidence angle from the desired signal (compared to the same interference and desired signal directions). The results also show that as the angular spread increases, the reduction of the BER between the two cases reduces (the curves moves together), indicating that the angular spread is wide enough so the array is able to separate the interferers from the desired signal. In both cases, the center arrays has the worst performance, followed by the corner arrays with independent beamforming and then the best performance from the corner arrays with combined beamforming.

In Figure 64 and Figure 65 the interferers are offset by 10° and 15° respectively on either side of the incidence angle of the desired signal. There is a significant improvement in the BER when the interferers move from 0° to 10°, but less so when they move between 10° and 15°

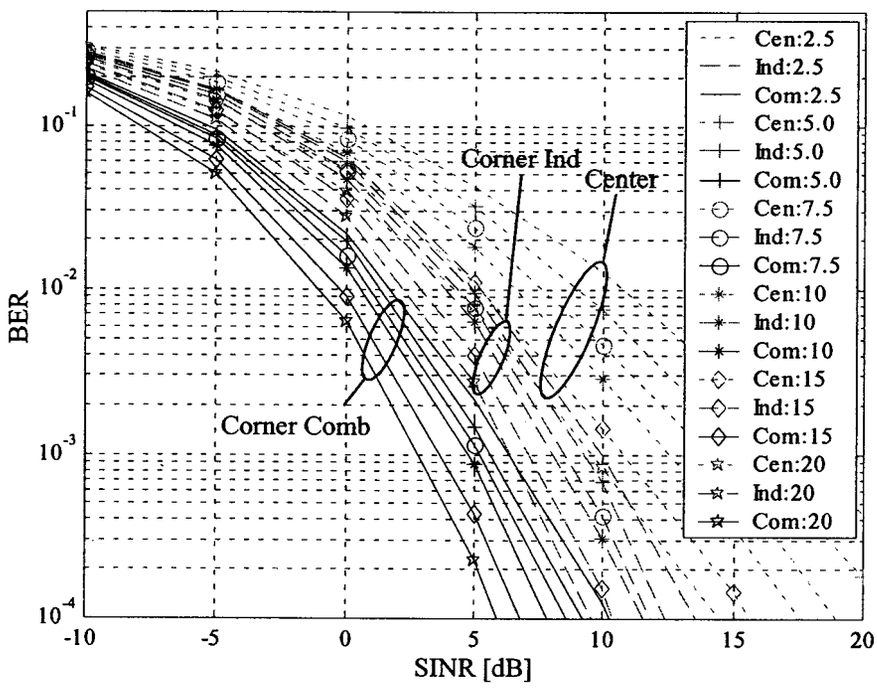

Figure 62: BER as a function of the SINR and angular spread of four element arrays with two equal strength interferers in the same direction as the desired signal.

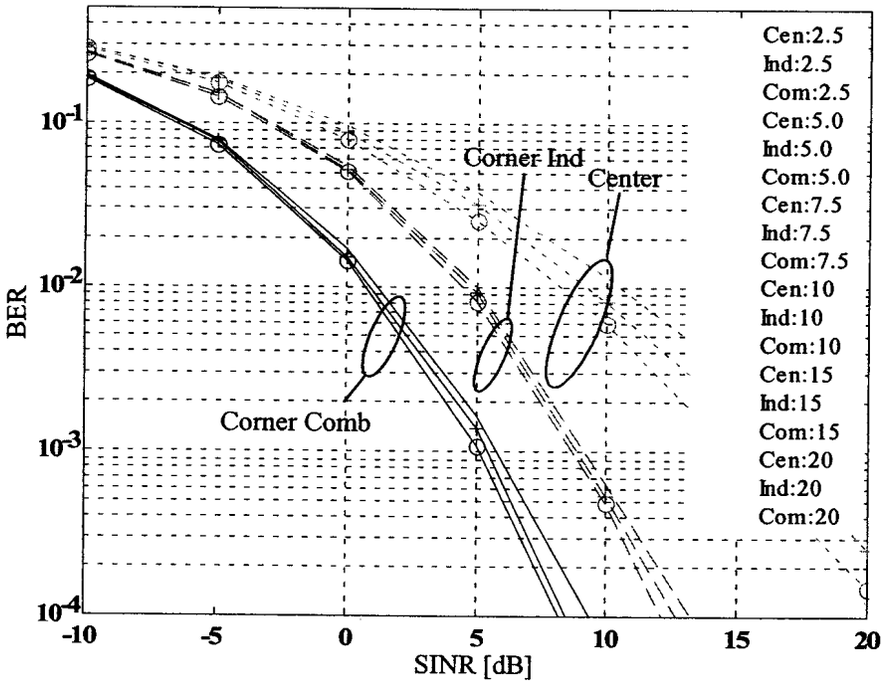

Figure 63: BER as a function of the SINR and angular spread of four element arrays with two equal strength interferers that are 5° offset in angle relative to the desired signal angle.

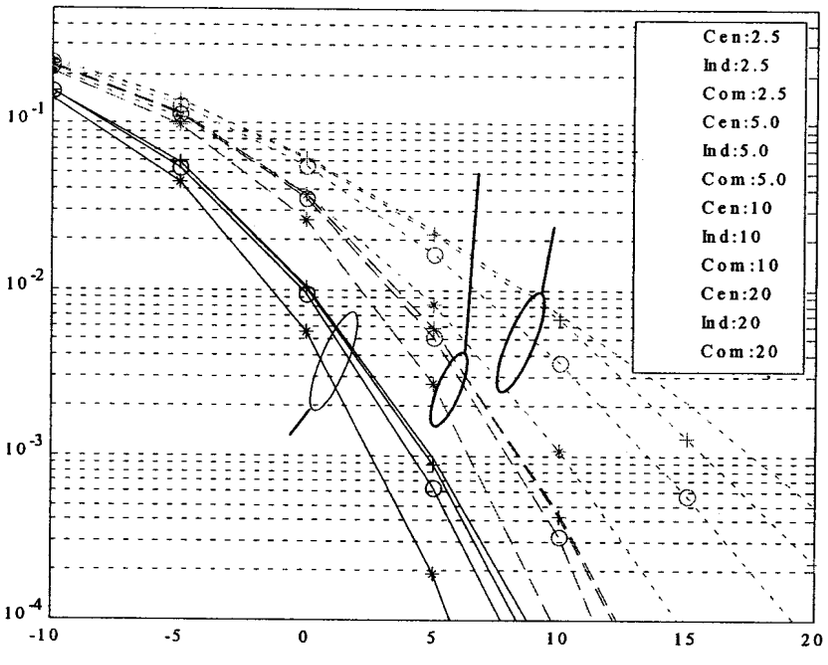

Figure 64: BER as a function of the SINR and angular spread of four element arrays with two equal strength interferers that are 10° offset in angle relative to the desired signal angle.

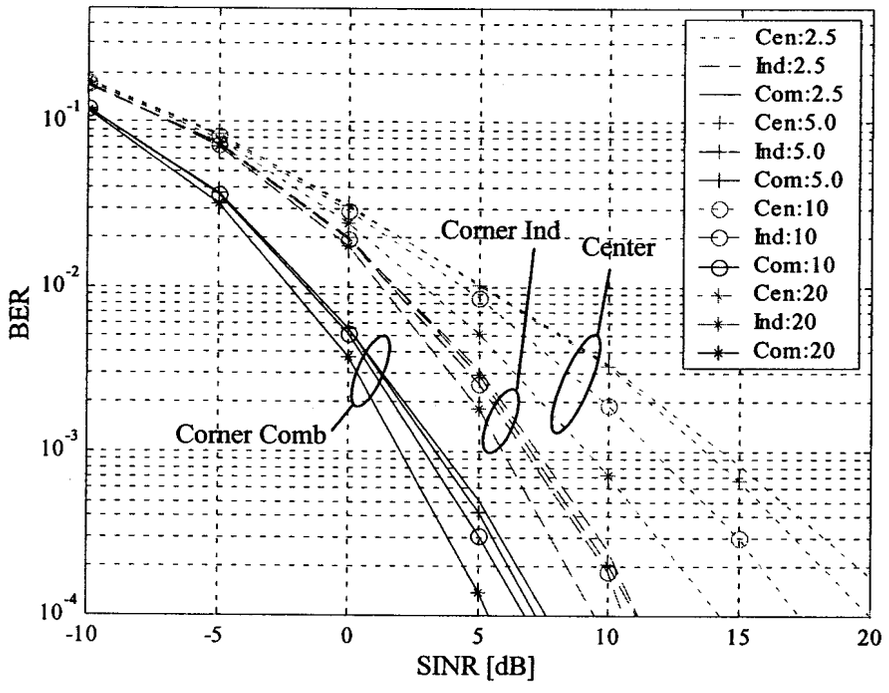

Figure 65: BER as a function of the SINR and angular spread four element arrays with two equal strength interferers that are 15° offset in angle relative to the desired signal angle.

The BER of a single cell with a uniform mobile distribution is shown in Figure 66 for a 2.5° angular spread, and Figure 67 for 5° and 10° angular spreads. The number of array elements is four and two equal strength interferers are present. It can be seen in Figure 66 that the BER is lower for the distributed array with combined beamforming compared to the distributed array with independent beamforming. For example at a SINR of 0dB, the BER of the arrays with combined beamforming is three times lower than the arrays with independent beamforming. The conventional center array has the same BER as the distributed array with independent beamforming, as can be expected. In Figure 67 it is shown that the BER is not significantly affected by angular spread, but it does decrease with larger (5° vs. 10°) angular spreads.

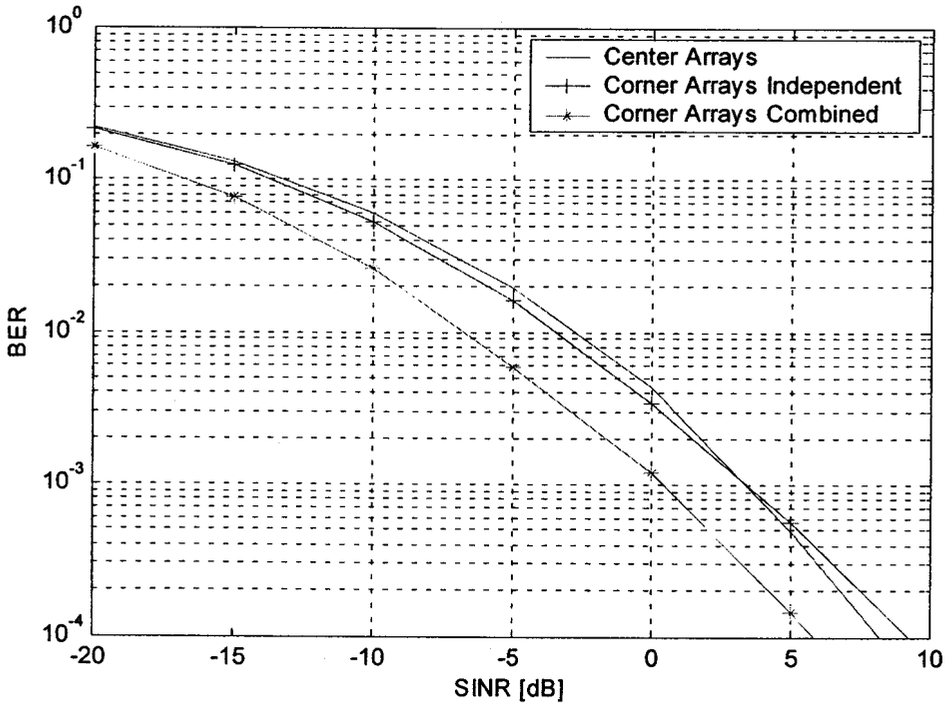

Figure 66: BER as a function of the SINR for conventional center arrays and distributed arrays with independent and combined beamforming with four elements per array and two interferers. The angular spread is 2.5° and the mobile positions is random within the cell.

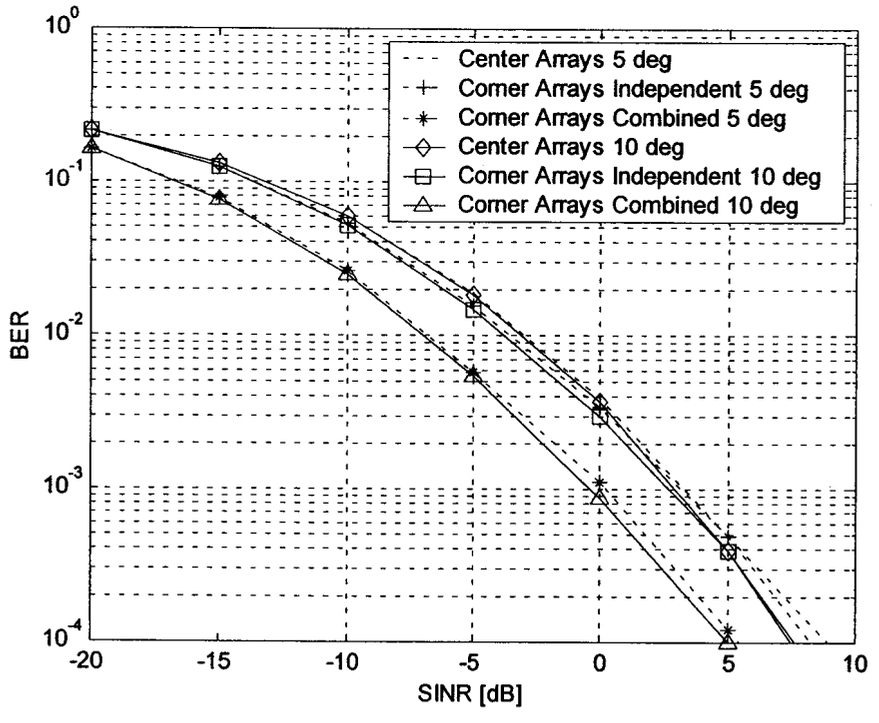

Figure 67: BER as a function of SINR for conventional center arrays and distributed arrays with independent and combined beamforming with four elements per array, two interferers, single cell, 5° and 10° angular spread and mobile positions random within the cell.

6.3.2 Slow Fading

In this section the effect of slow fading on the outage probability of conventional center arrays and corner distributed arrays is examined. The formulation for slow fading is given in section 2.4.2. In order to focus on the effect of slow fading, fast fading will initially be excluded. Slow fading can partially be compensated for by careful control of the basestation and mobile transmit powers. The amount of slow fading compensation in the downlink depends on the maximum available BTS power and mobile sensitivity, and on the uplink on the maximum available mobile transmit power and BTS receiver sensitivity. Slow fading in a multi-basestation configuration (or distributed arrays) can only be compensated for one of the basestations if a single slot in TDMA is used for simultaneous reception by all the basestations. Multi-timeslots can be used to compensate for slow fading to multiple base stations operating in optimum combining mode (see 2.5.4.3).

The effect of fast fading is typically investigated by looking at the bit error rate as was done in the previous section [2,24]. The effect of slow fading is typically investigated by looking at the outage probability [12,38]. The outage probability is the probability that the received SINR is less that a certain protection ratio. The protection ratio is the minimum tolerable carrier to interference ratio for a specific bit error (or frame error) rate performance. The required protection ratio for GSM is 3dB [22].

In order to verify the slow fading method used in this thesis, a Monte-Carlo simulated outage probability result was compared with the outage probability given in [37]. The outage probability for a single element (sectorized) antenna at the center of the cell as well as cell corner distributed sectorized antennas[42] is shown in Figure 68. The slow fading standard deviation is 6dB, the pathloss coefficient is 3.5 and the angular spread is 0°[43]. A network with 37 cells and reuse factor of 3 with one co-channel user per cell was used. In order to compare macro-diversity[44] systems with conventional systems, an interferer

[42] Sectorized antennas located at alternate corners of the cell.
[43] All multipath components have the same incidence angle at the base station antenna.
[44] Macro diversity is a term used for antennas spaced far apart, with uncorrelated (or low correlation) slow fading between then.

activity of 75%[45] was assumed [37]. The outage probability for maximum ratio combing of the corner element signals was calculated based on the approximation given in [37,63]:

$$\mathrm{Prob}_{MRC}(\mathrm{SINR} \le \mathrm{SINR}_o) = \mathrm{Prob}\left(\sum_{\kappa=1}^{3}\mathrm{SINR}_\kappa \le \mathrm{SINR}_o\right) \qquad (191)$$

where SINR_κ is the carrier to interference ratio of corner distributed antenna κ and SINR_o is the protection ratio. The outage probability of combined optimum beamforming of the corner antenna signals (see section 2.7) is also shown in Figure 68. Optimum combining is equivalent to maximum ratio combining in the absence of interferers [2]. Since interferers are present in the calculation, the maximum ratio combining approximation given in [37] is therefore actually an optimum combining approximation.

The calculated results shown in Figure 68 for the center and corner antennas are in close agreement with the results presented in [37], indicating an accurate simulation procedure. In addition, the results indicate a close agreement between the calculated outage probability of optimum combining and maximum ratio combining (which can be expected as described above). It is important to note that the outage probability of a single BTS receiver is higher than that of a multi-BTS optimum combining (or maximum selection) receiver. This is the principle of macro diversity or diversity against shadowing [63]. Macro diversity is used in all CDMA and UMTS systems in handoff (called soft handoff to multi-BTSs as opposed to hard handoff to a single BTS in TDMA systems) [56, page 137, 40]. It is stated in [56, page 137] that the required Eb/No (energy per bit divided by the noise spectral density) is 3dB lower when macro-diversity is applied.

In the next part of this section, the outage probability as a function of the number of antenna elements of conventional center and corner distributed arrays will be investigated. Initially a reuse factor of 3 will be used, with one element per array. Thereafter, the number of users per cell will be increased. This will be followed by an investigation of the outage probability with a cell reuse factor of one and one or more co-channel users per cell.

[45] Means that 25% of the interferers was inactive during each simulation iteration.

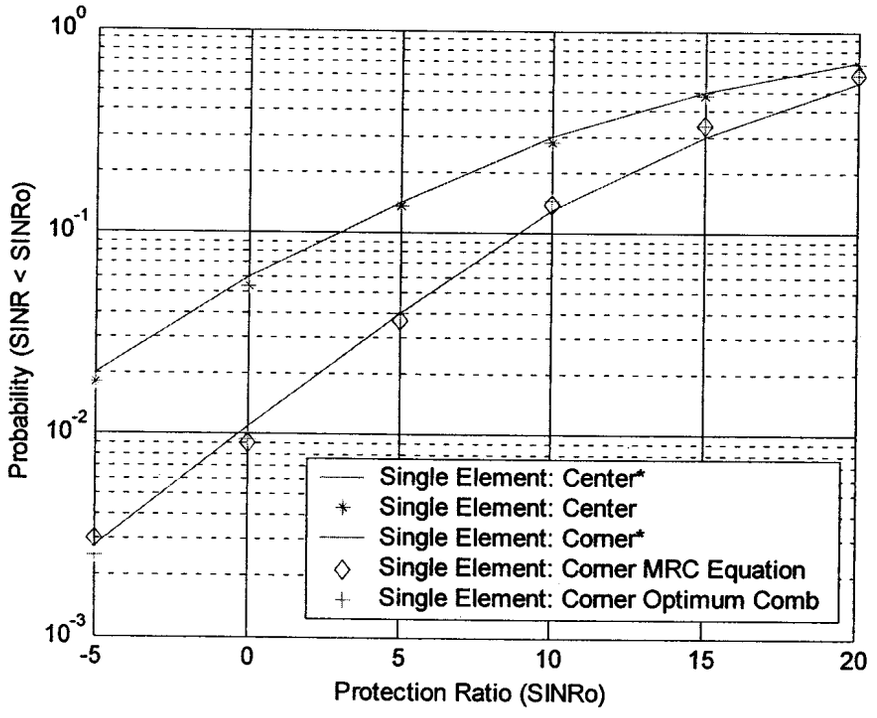

Figure 68: Comparison of simulated outage probability with results in [37] for a single element center antenna as well as corner cell antennas. *From reference [37].

The outage probability for one, two and four element arrays at the center and corners of the cell is shown in Figure 69. The angular spread is 0°, a 37 cell network is used and the reuse factor is 3. The corner array signals are combined in two ways:

1. Optimum beamforming for each corner array followed by approximate optimum combining of all three corner arrays (see equation 191),
2. Full optimum combined beamforming of all three corner arrays,

The results indicate that combined beamforming has a lower outage probability than individual array beamforming. As an example, for an outage probability of 1E-2, combined beamforming requires approximately 2.25dB lower carrier to interference ratio than individual beamforming of the two element arrays and 3.5dB for the four element arrays. In addition, for the same outage probability, the required CIR is approximately 6.5 and 7.0dB lower for the corner arrays with combined beamforming than the conventional array at the cell center, for two and four element arrays respectively.

The outage probability for one same-cell co-channel interferer is shown in Figure 70 for 0° angular spread with 2 and 4 element arrays. Comparing the outage probability in Figure 69 and Figure 70, it can be seen that the outage probability is higher in the case of a co-channel interferer located in the same cell as the desired signal (as can be expected).

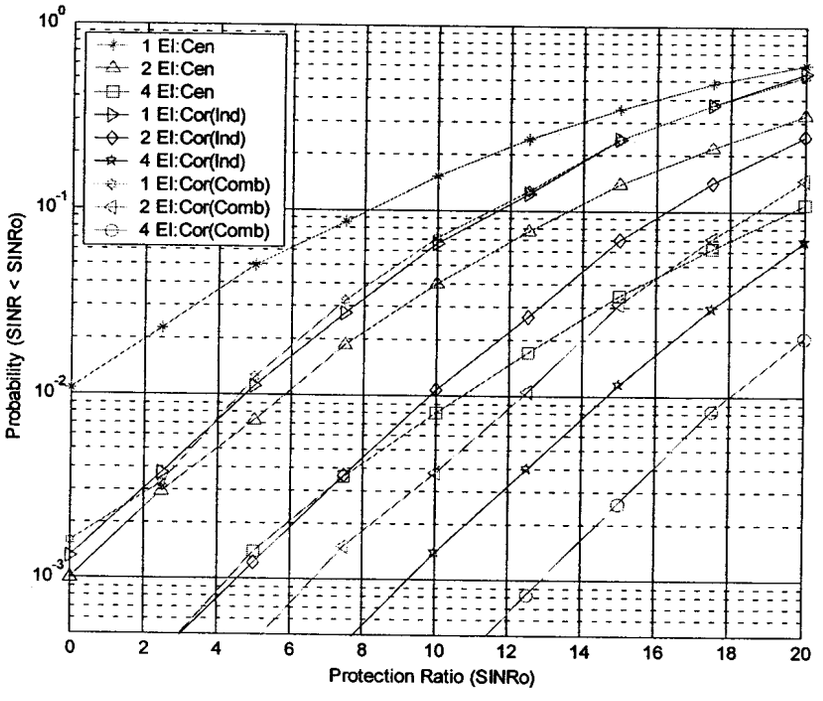

Figure 69: Outage probability as a function of protection ratio for one, two and four element arrays in the center and corners of a cell for a 37 cell network with a reuse factor of three.

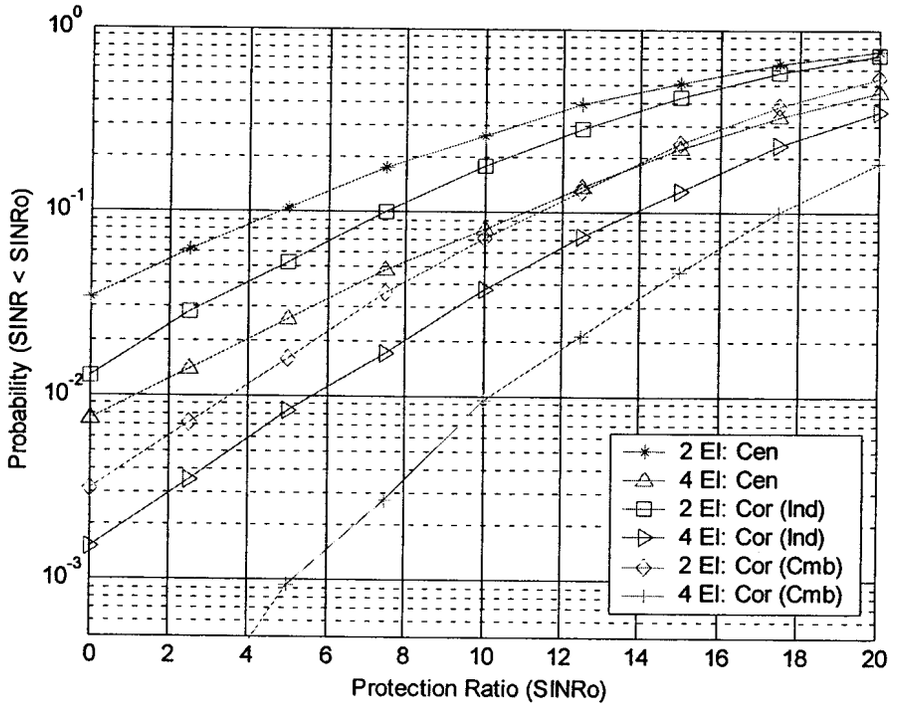

Figure 70: Outage probability as a function of protection ratio and number of elements for center, corner individual and combined beamforming arrays and with one same cell interferer and zero degree angular spread. A 37 cell network with a reuse factor of three is used.

The outage probability for two and four element arrays is shown in Figure 71 for 0° and 5° angular spread and Figure 72 for 5° and 10° angular spread. The figures indicate that there is a slight decrease in the outage probability for 5° angular spread relative to 0°. However the outage probability is similar for the 5° and 10° angular spread cases, indicating that the improvement in outage probability reduces as the angular spread exceeds a certain value (5° in this case).

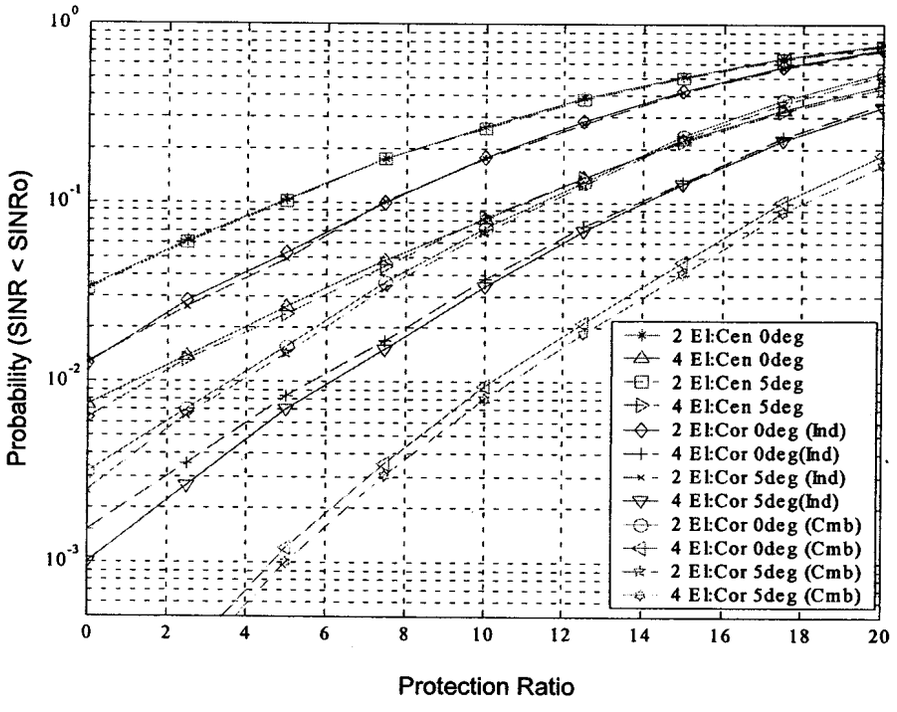

Figure 71: Outage probability as a function of protection ratio, number of elements and angular spread (0° and 5°) for center and corner arrays with independent and combined beamforming with one same-cell interferer. A 37 cell network with a reuse factor of three is used.

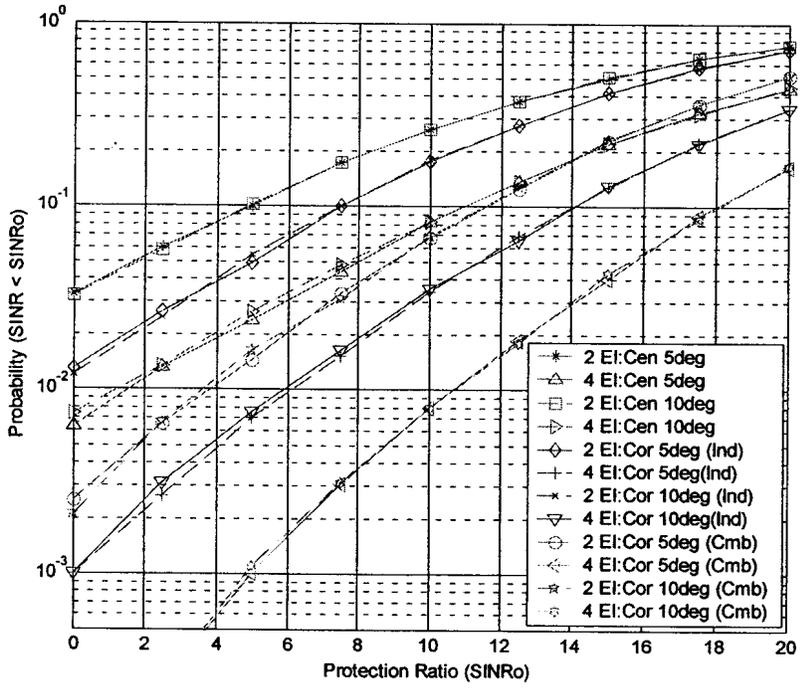

Figure 72: Outage probability as a function of protection ratio, number of elements and angular spread (5° and 10°) for center and corner arrays with independent and combined beamforming with one same cell interferer. A 37 cell network with reuse factor of three is used.

The outage probability as a function of the number of same-cell co-channel interferers (one and two interferers) is shown in Figure 73 for four element arrays and an angular spread of 5°. The figure indicates that the outage probability for the corner arrays with combined beamforming is lower than the outage probability for the center and corner arrays with individual beamforming.

In the case of two interferers and for a 1% outage probability, the combined beamforming array can sustain a protection ratio of 6.5dB vs. 0.8dB for the corner arrays with individual beamforming and –2.5dB for the center arrays.

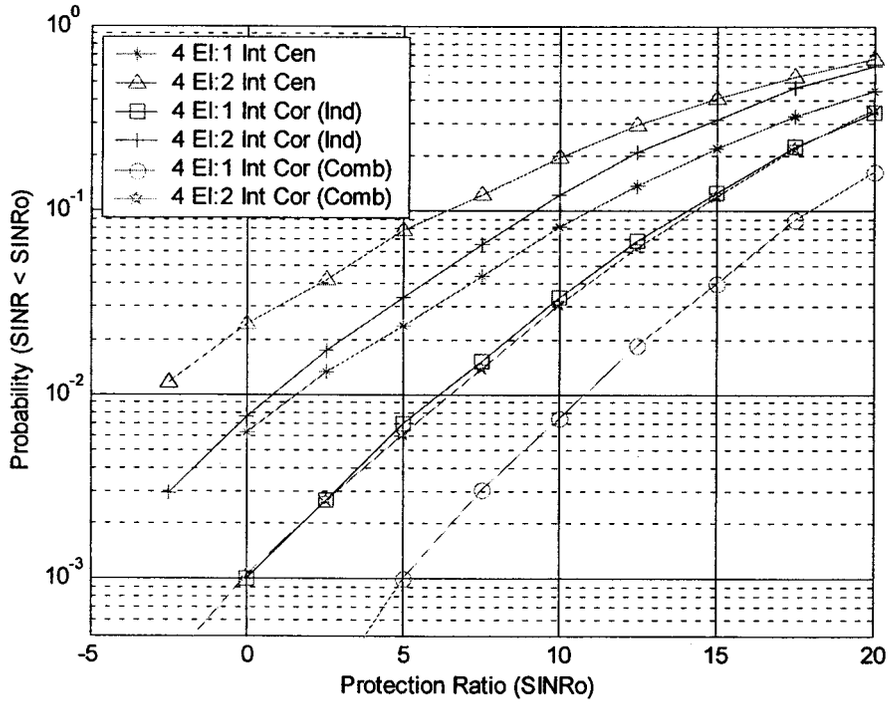

Figure 73: Outage probability as a function of protection ratio, number of same-cell co-channel interferers and array type (center, corner arrays with independent and combined beamforming) with the following conditions: 37 cell network, reuse factor of three, 5° angular spread and four element arrays.

6.3.3 Slow and Fast Fading

In this section the outage probability performance of the array systems in the center (conventional), corner with individual and combined beamforming for both fast and slow fading will be investigated. The loading for the conventional network will be equal to the

networks with arrays at the cell edges[46]. The slow fading standard deviation is 8dB, which is a typical value used in simulations [8,22,42].

According to [22] the average SINR for GSM to provide a reasonable voice quality is 9dB for a Rayleigh fading channel. The required instantaneous SINR of the receiver is 3dB. The simulation results in [22, p.112] show that the outage probability of a conventional three sector GSM system with a reuse of three, slow fading standard deviation of 8dB and pathloss exponent of 3.5 is 2.2%. According to equation 4.4 in [22], the equivalent outage probability (using equation 191) is 20% lower, or approximately 1.83%. A target performance of 2% outage probability is typically required [33, page 1504]. The minimum protection ratio $SINR_0$ that is used in the capacity simulations in [34, p.2057] is 9dB.

The outage probability for one same-cell co-channel interferer is shown in Figure 74 for a four element array and reuse of 3. The shadow fading standard deviation is 8dB and pathloss exponent is 3.5. The power is controlled by the sub-array closest to the mobile (range based power control).

[46] Note that in the previous section the conventional network was loaded 25% lower than the network with base stations at the cell edges [37].

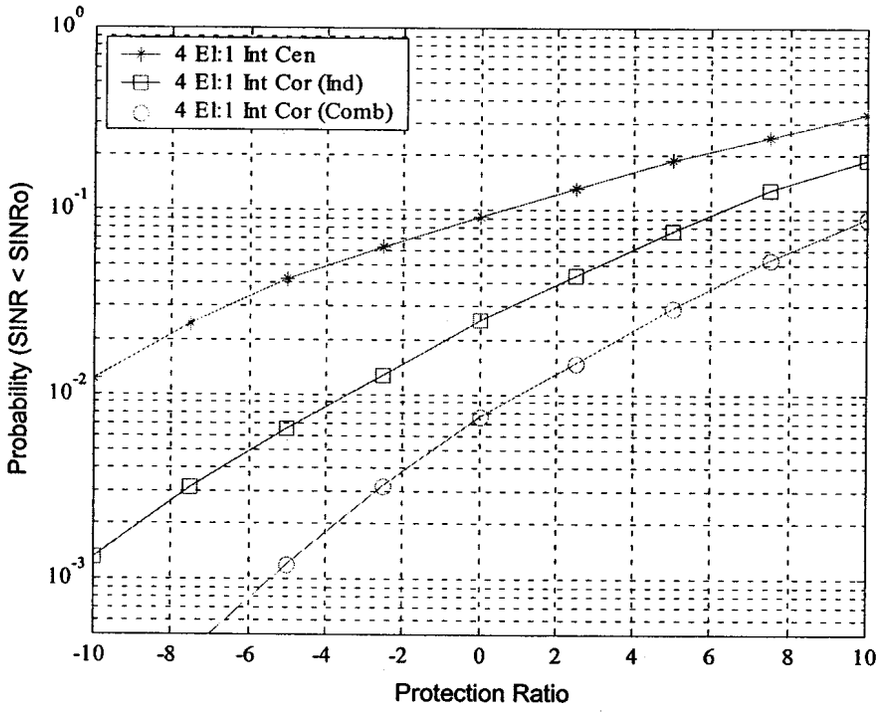

Figure 74: Outage probability as a function of protection ratio and array type (center, corner independent and combined beamforming arrays) with the following conditions: Fast and slow fading, one same-cell co-channel interferer, 4 element arrays, 5° angular spread, 19 cell network, reuse of three and range based power control.

The outage probability as a function of the number of co-channel interferers is shown in Figure 75 for a four element array and reuse of 3. The shadow fading standard deviation is 8dB and pathloss exponent is 3.5. The power is controlled by the sub-array (in the cell containing the desired signal) receiving the maximum signal (receive signal power control). This means that the power of the mobile is adjusted to normalize the slow fading and pathloss between mobile and sub-array receiving the maximum signal. Fast fading power control, such as is used in CDMA, was excluded. Comparing Figure 74 to Figure 75, it can be seen that the outage probability is higher for range based power control. This is because the slow fading is effectively cancelled by increasing the transmit power in received signal based power control.

The results show further that the corner arrays with independent beamforming and two (almost three) same-cell co-channel users (one co-channel interferer) can satisfy the GSM criteria of a protection ratio of 3dB and outage probability of 1.8%. This means that the system capacity is effectively doubled for a reuse of 3. The corner arrays with combined beamforming can support three (almost four) same-cell co-channel users (three co-channel

interferers), thus effectively tripling the capacity for a reuse of 3. The arrays at the cell center is not able to meet the GSM criteria for more than one co-channel same cell user with a four element array.

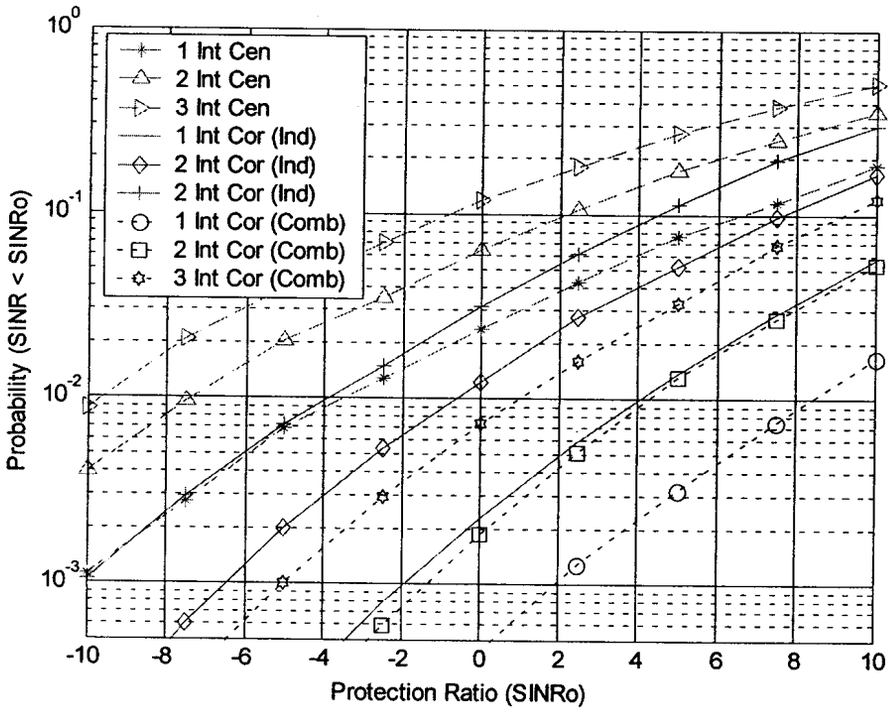

Figure 75: Outage probability as a function of protection ratio and array type (center, corner independent and combined beamforming arrays) with the following conditions: Fast and slow fading, one to three same-cell co-channel interferers, four element arrays, 5 ° angular spread, 19 cell network, reuse of three and received based power control.

The outage probability for a reuse pattern of one and four element arrays for one and two interferers is shown in Figure 76. The same frequency is now reused in all the cells, which leads to an extremely high out of cell interference. This out of cell interference will in turn increase the outage probability (compared to a reuse of 3), which is confirmed by the results in Figure 76. Only the corner array with combined beamforming and one same cell co-channel interferer meets the GSM criteria of outage probability of 1.83% with protection ratio greater than 3dB. This means that with the combined beamforming corner array two same cell co-channel users can be sustained for a four element array, doubling the capacity in a network with a reuse pattern of one.

The outage probability for a reuse pattern of one, six element arrays and one to three interferers is shown in Figure 77. The results indicate that two same cell co-channel users for the corner arrays with independent beamforming and three same cell co-channel users

with the corner arrays with combined beamforming can be supported for the GSM criteria. This is double and triple capacity increases for the corner arrays with independent and combined beamforming, respectively.

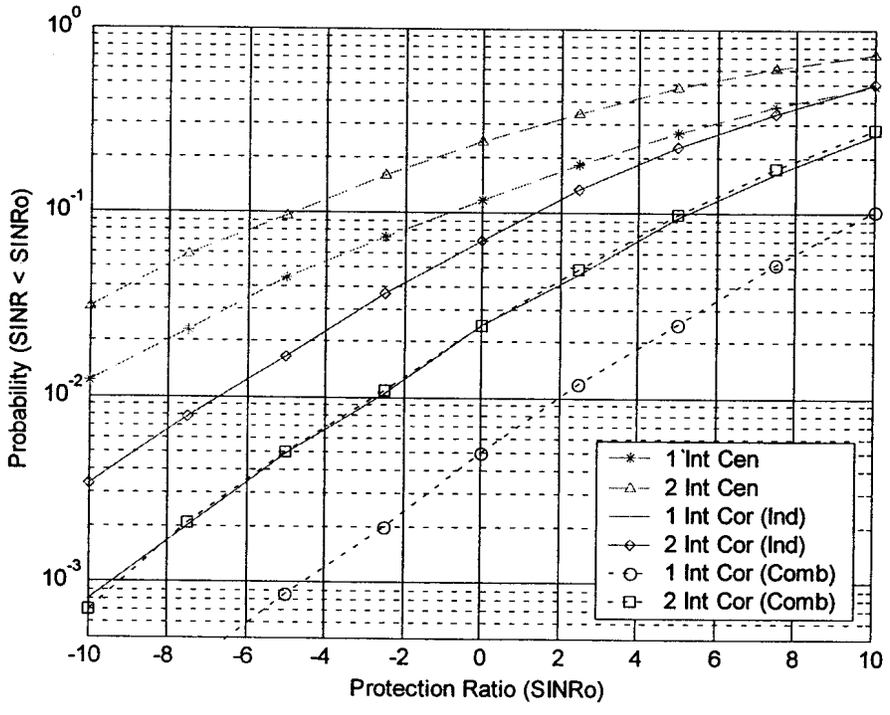

Figure 76: Outage probability as a function of protection ratio and array type (center, corner independent and combined beamforming arrays) with the following conditions: Fast and slow fading, one and two same-cell co-channel interferers, four element arrays, 5° angular spread, 19 cells, reuse factor of one and received based power control.

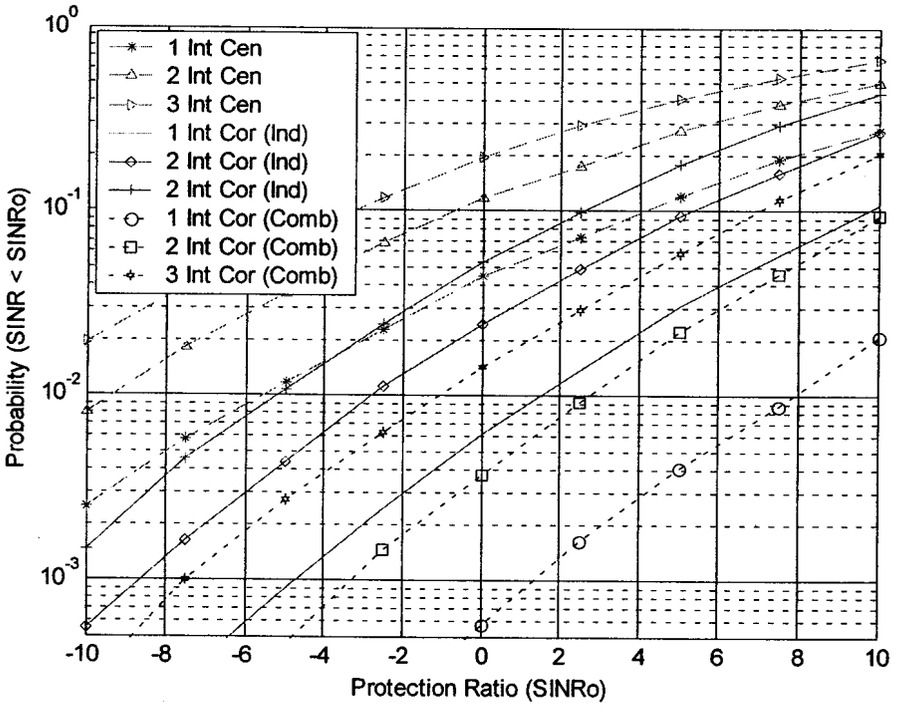

Figure 77: Outage probability as a function of protection ratio and array type (center, corner independent and combined beamforming arrays) with the following conditions: Fast and slow fading, one to three same-cell co-channel interferers, six element arrays, 5° angular spread, 19 cells, reuse factor of one and received based power control).

Thus it is shown how the outage probability is reduced and capacity is increased by increasing the number of array elements. The capacity can be improved further by increasing the number of elements even further. However, practicality limits the maximum array size and thus number of antenna elements. The antenna size is mainly limited by two main factors. Firstly, larger arrays have more wind loading than the single element antennas. Secondly, the antennas are installed on towers and buildings. In order for an operator to get approval to install the antenna, it has to have a minimum visual disturbance. Therefore, operators want to minimize the antenna size. A six element array at 1900MHz is approximately 0.55m wide, which is 3.5 times wider than the standard antenna. This is probably the size limit. Therefore, from a practical point of view the study in this thesis will not cover antenna arrays exceeding 6 elements.

6.4 Conclusions

In this chapter the bit error rate (BER) and outage probability of adaptive arrays was estimated with a Monte-Carlo method as a function of the angular spread, propagation channel model, antenna element spacing, number of interferers and angular separation

between signals. Firstly, it was shown that the BER is reduced significantly in a narrow angular spread environment, if the elements are spaced far apart (5λ vs. 0.5λ), even if the desired signal and the interferers are in the same direction.

The BER (without slow fading) of 0.5λ element spaced conventional arrays and distributed arrays with independent and combined beamforming was compared as a function of the angular spread and separation in angle between the desired signal and the interferers. It was shown that the BER of the distributed array with combined beamforming is lower than the BER of distributed array with independent beamforming, and that the BER reduces as the angular spread increases. The BER of the distributed array with independent beamforming is similar to the BER of the conventional center cell arrays.

The outage probability, including the effect of slow fading, was compared between the distributed array with combined and independent beamforming as well as conventional arrays at the cell center for multiple same-cell co-channel users in a 19 cell network with 0.5λ element spacing. The results indicate that two same cell (frequency reuse of one) co-channel users can be supported by six element distributed arrays with independent beamforming, while three same-cell co-channel users can be supported with a six element distributed array with combined beamforming in a GSM cellular network, where the angular spread is 5°.